Optical readout method based on time-discrete modulation for micro-cantilever array sensing

Xuhong Chu (褚旭红)[1], Liquan Dong (董立泉)[1],*, Yuejin Zhao (赵跃进)[1], Xiaomei Yu (于晓梅)[2], and Yun Feng (冯 韵)[1]

[1]*Beijing Key Lab. for Precision Optoelectronic Measurement Instrument and Technology, School of Optoelectronics, Beijing Institute of Technology, Beijing 100081, China*
[2]*Institute of Microelectronics, Peking University, Beijing 100087, China*
*Corresponding author: kylind@bit.edu.cn

Noise and the resonance characteristics of the focal plane array (FPA) are the most important factors that affect the performance of the optical readout infrared (IR) FPA imaging system. This Letter presents a time-discrete modulation technology that eliminates the background and restrain noise, which effectively improves the image quality of the optical readout IR FPA imaging system. The comparative experiments show that this technology can reduce the noise equivalent temperature difference greatly and make the images sharper. Moreover, when the imaging system is influenced by the environment vibration, the images obtained from the imaging system with time-discrete modulation restore twice as fast as without time-discrete modulation.

OCIS codes: 110.3080, 110.2970, 040.6808, 100.2550.
doi: 10.3788/COL201614.101102.

Since the practical applicability of the optical readout infrared (IR) focal plane array (FPA) imaging system was confirmed, much attention has been paid to this technology due to its advantages of small volume, light weight, and low power[1], and it is predicted that this imaging technology will be widely applied in the future[2–6]. Compared with the cooled IR imaging system and the electric readout IR FPA imaging system, the optical readout IR FPA imaging system is immature at this moment, and its performance indexes have great disparity from the theoretical results. So, many research institutes have carried out much research on the optical readout IR FPA imaging system using the bi-material micro-cantilever detector. Some research related to optimizing the imaging system to improve the detection sensitivity of the optical readout system, such as improving the implementation of the optical path[7], selecting the filter[8], analyzing and compensating the manufacturing defect[9,10] of the FPA, etc. Other research is focused on developing new forms of the readout system to decrease its dependence on environment and to improve the reliability of the imaging system, such as fiber-reference optical readout technology[11].

The noise equivalent temperature difference (NETD) of the optical readout IR FPA imaging system can be theoretically reduced to less than 5 mK, however, it is usually almost 120 mK or more in practice, which may be due to the fact that there are many factors that could degrade the image quality[12–14]. These factors contain the noise generated from the FPA, the optical system, and the environment. The time-discrete modulation technology is proposed to compensate the noise of the FPA and the noise of the environment. Experiment results show that this technology can not only improve the image contrast, but recover the image effect more quickly than without

time-discrete modulation when the imaging system undergoes vibration.

The FPA is the main detector of the imaging system, which consists of bi-material cantilever arrays, as shown in Fig. 1. It is an array of the same bi-material micro-cantilever structural units and each structural unit is called a pixel, as shown in Fig. 1(a). The absorber/reflector structure of each pixel has one layer as an IR absorber made of SiN_x, and the other layer as a visible light reflector made by Au, as shown in Fig. 1(b)[15]. Each pixel's micro cantilevers of the FPA do not deform when there is no IR radiation focused on it, but the cantilevers will deflect when the FPA absorbs the IR thermal radiation due to the difference between the thermal expansion coefficients of the two layer materials. The deflected angle θ of each pixel is proportional to the absorbed radiation focused on it, namely, different IR radiations from different object points will make different deflected angles θ.

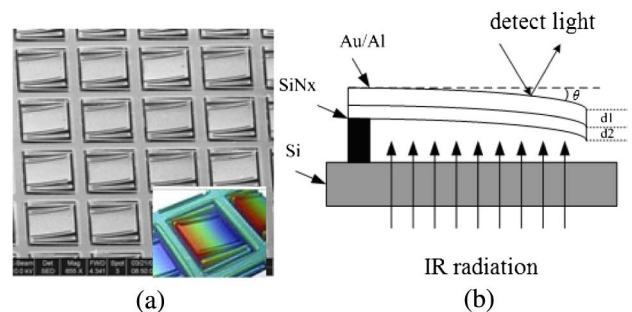The structure of the time-discrete modulation optical readout IR FPA imaging system is shown in Fig. 2.

Fig. 1. (a) FPA and its pixel and (b) the bi-material micro-cantilever structure of an FPA pixel.
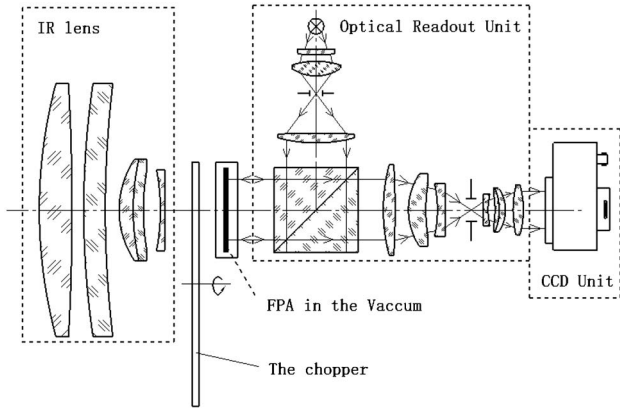
Fig. 2. Time-discrete modulation optical readout IR FPA imaging system.

It consists of five parts: the IR lens, the FPA in a vacuum, the optical readout unit, the imaging unit, and the chopper. Compared with the typical optical readout IR FPA imaging system, the key point of the current system is that a chopper is used to modulate the radiation.

In the typical optical readout IR FPA imaging system, the IR lens collects the IR thermal radiation from the target object and focuses them on the FPA, which is placed in the vacuum chamber. Then the pixels of the FPA produce thermomechanical deformation according to the absorbed radiation. The optical readout unit detects and exports the thermomechanical deformation of each pixel of the FPA by a noncontact measuring method. In the optical readout unit, the light emitted from the light source is collimated by its illumination lens, then directed to the FPA for optical imaging. The rays reflected by the FPA are focused on the filter plane, and then the filtered beam is projected onto the CCD by the imaging lens. The energy that the CCD receives is E_0 when there is no deformation of the FPA, and it will change to E_t when the FPA deflects due to the object IR radiation. Then the energy variation that the CCD detects can be calculated as $\Delta E = E_0 - E_t$. The image processing system receives and displays ΔE on the monitor in the form of gray-level difference.

If ΔE is caused not only by the object IR radiation but other noise, such as the vibration and the fluctuation of the light source intensity, the image of the imaging unit will not be real. In order to get the energy variation caused by the object IR radiation only, the noise must be deducted. The chopper is employed to deduce the effect of noise on ΔE and improve the image quality of the system.

According to Fig. 2, there are two links to bring noise into the imaging system. One is mainly caused by FPA during the process of converting the IR radiation to the angle deflection of the FPA. The other is the optical readout system during the process of converting the angle deflection of the FPA to the visible energy variation. The latter has been analyzed in Ref. [8] and compensated by using the fiber reference technology. This Letter focuses on the FPA noise.

The structure characteristics of the micro cantilever always cause three intrinsic noises, namely, background fluctuation noise (NETD_{bf}), temperature fluctuation noise (NETD_{tf}), and thermomechanical noise (NETD_{tm}). The total noise is expressed as[16],

$$\begin{aligned}
&\text{NETD}_{\text{total}} \\
&= (\text{NETD}_{\text{tf}}^2 + \text{NETD}_{\text{bf}}^2 + \text{NETD}_{\text{tm}}^2)^{1/2} \\
&= \left(\frac{8F^2 T_D \sqrt{k_B B G}}{\eta \tau_0 A_D (dP/dT)_{\lambda_1 - \lambda_2}} + \frac{8F^2 \sqrt{2k_B \sigma B (T_D^5 - T_B^5)}}{\eta \tau_0 (A_D)^{1/2} (dP/dT)_{\lambda_1 - \lambda_2}} \right. \\
&\quad \left. + \frac{8F^2 \sqrt{k_B B T_D / k_S Q \omega}}{\eta \tau_0 S_T (dP/dT)_{\lambda_1 - \lambda_2}} \right)^{1/2}.
\end{aligned} \tag{1}$$

These noises can superimpose on the deflection angle θ of the FPA, namely,

$$\theta_0 = \theta_{0\,\text{read}} + \theta_{0\,\text{noise}}, \tag{2}$$

$$\theta_t = \theta_{t\,\text{read}} + \theta_{t\,\text{noise}}, \tag{3}$$

where $\theta_{0\,\text{real}}$ is the deflection angle of the FPA when there is no IR radiation and $\theta_{0\,\text{noise}}$ is caused by the noise of the FPA at this time; $\theta_{t\,\text{real}}$ is the deflection angle when there is IR radiation and no noise and $\theta_{t\,\text{noise}}$ is caused by the noise of the FPA at this same time.

The deflection $\Delta\theta_{\text{real}}$ caused by the object radiation can be expressed as

$$\Delta\theta_{\text{real}} = \theta_{0\,\text{read}} - \theta_{t\,\text{real}}. \tag{4}$$

Substituting Eqs. (2) and (3) into Eq. (4), we get

$$\begin{aligned}
\Delta\theta_{\text{real}} &= \theta_{0\,\text{read}} - \theta_{t\,\text{real}}, \\
&= (\theta_0 - \theta_{0\,\text{noise}}) - (\theta_t - \theta_{t\,\text{noise}}), \\
&= (\theta_0 - \theta_t) - (\theta_{0\,\text{noise}} - \theta_{t\,\text{noise}}), \\
&= \Delta\theta - \Delta\theta_{\text{noise}}, \tag{5}
\end{aligned}$$

where $\Delta\theta$ can be measured by the system; $\Delta\theta_{\text{noise}}$ is directly related to the access time of t and t_0. When t is infinitely close to t_0, $\Delta\theta_{\text{noise}}$ will inevitably be close to 0.

Under normal circumstances, the system collects the initial deflection angle of the FPA θ_0 at time t_0, and θ_t at time t. $\Delta\theta_{\text{noise}}$ will increase over t, which results in $\Delta\theta$ increasingly deviating from $\Delta\theta_{\text{real}}$. This will lead to the degradation of the system performance, including the detection sensitivity and image authenticity.

Besides the noises of the FPA directly reducing the NETD and other indexes of the optical readout IR FPA imaging system, the imaging quality is also seriously affected by the vibration outside because of the resonance characteristics of the micro cantilevers, which will cause the system to not be able to form images or even invalidation. The intrinsic noise and the response to the outside vibration are restricted by the FPA principle, and they cannot be eliminated thoroughly. Thus, certain devices

and image processing progress are necessary to reduce or compensate these unwanted effects on the system performance.

Time-discrete modulation technology is presented to eliminate the intrinsic noise of the FPA and the influence of the outside vibration, which contains two steps.

First, the continuous IR radiation from the target object is modulated to a discrete one, namely, time-discrete modulation. This process relies mainly on the mechanical chopper that is inserted between the IR lens and the FPA that can modulate the continuous IR radiation signal to a discrete one. The chopper is divided into two opaque regions and two transmission regions that are alternately placed, as shown in Fig. 3.

In the working process, the mechanical chopper rotates at a certain frequency. Thus, the transmission area and the opaque area enter the optical path alternately over time. When the opaque region of the chopper is in the optical path, what the signal CCD receives is the noise of the FPA; when the transmission region of the chopper is in the optical path, what the signal CCD receives is the object signal containing the noise of the FPA. That is to say, the rotating mechanical chopper makes the IR radiation that the FPA receives from the target become a cyclical signal over time. We make the initial deflection angle of the FPA θ_0 at time t, and θ_t at time $(t+1)$, hence, according to Eq. (5), $\Delta\theta$ will be closer to $\Delta\theta_{real}$ because of the reduction in $\Delta\theta_{noise}$.

Second, the CCD unit receives and demodulates signals from the optical readout unit, then the IR image is output correctly. The discrete signals that the CCD receives contain interval image signals with noise and the noise signals. After distinguishing the two kinds of signals, the noise signals are deducted from the image signals with noise, therefore quality images are output. By deducting the noise from the image, not only can the SNR and the detection sensitivity of the system be improved directly, but the high-quality image can be gained.

There are many factors that affect the feasibility of the imaging system. The first and most important one is the frame synchronization of the chopper and the CCD, which ensures that the integration of the CCD signal frame can be achieved in the transmission/opaque region of the chopper. Otherwise, the signals that the CCD receives are not periodic and the noise cannot be eliminated. The second one is that the response time of the FPA must be much smaller than the integration time of the CCD. Otherwise, even if the opaque region of the chopper is
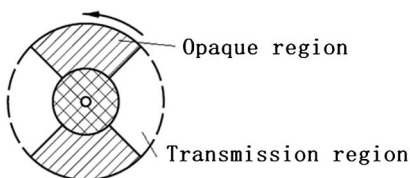
in the light path, the signal the CCD receives shall contain the object radiation because of the response lag of the FPA, which makes the modulation invalid. The third one is that the starting point of the integration time of the CCD must be synchronized with the transmission/opaque region of the chopper. Otherwise, the intensity of the image signal will be reduced even though the image signal is modulated, making the modulation lose its effect.

To verify the imaging effect of time-discrete modulation optical readout technology, the experiment system is set up according to Fig. 2. In the system, the chopper wheel and its motor drive unit are shown in Fig. 4.

Results of the comparative experiments are shown in Fig. 5.

Figures 5(a) and 5(b) are both captured by the optical readout IR FPA imaging system without time-discrete modulation. The illuminating energy of the optical readout system that serves Fig. 5(b) is twice that of Fig. 5(a), so the brightness of the image in Fig. 5(b) is much higher than that of Fig. 5(a). Figure 5(c) is captured by the imaging system according to Fig. 3.

The NETD is one of the key indexes that represent the detection sensitivity of the IR imaging system. It can be expressed as

$$\mathrm{NETD} = \Delta T \times \frac{V_n}{V_s}, \qquad (6)$$

where ΔT is the temperature difference, V_s is the peak voltage of the signal, and V_n is the RMS value of the noise.

We substitute G_{max}, the gray value of the image, and G_n, the noise gray value for V_s and V_n, and get

Fig. 4. Chopper wheel and its motor drive unit.

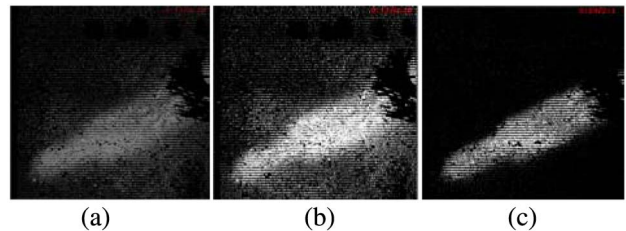(a)   (b)   (c)

Fig. 5. Images of a hot iron captured by the optical readout IR FPA imaging system (a,b) without time-discrete modulation and (c) with time-discrete modulation.

Fig. 3. Mechanical chopper.

Table 1. Calculated Values of NETD

	Fig. 5(a)		Fig. 5(b)		Fig. 5(c)	
	Value	Mean	Value	Mean	Value	Mean
$G_{\mathrm{max}1}$	98	98	163	165.3	160	161
$G_{\mathrm{max}2}$	92		176		156	
$G_{\mathrm{max}3}$	104		157		167	
G_{n1}	21	20	36	36.3	4.1	3.1
G_{n2}	24		30		2.3	
G_{n3}	15		43		2.8	
NETD	$\Delta T \times k$ $\times 0.204$		$\Delta T \times k$ $\times 0.219$		$\Delta T \times k$ $\times 0.019$	

$$\mathrm{NETD} = \Delta T \times \frac{V_n}{V_s} = \Delta T \times k \times \frac{G_n}{G_{\mathrm{max}}}, \qquad (7)$$

where k is a coefficient.

By picking parameters from Fig. 5, the corresponding value of NETD can be obtained, as shown in Table 1.

From Table 1, we can see that the NETD of Figs. 5(a) and 5(b) are basically the same regardless of whether the image brightness is high or low, and the NETD of Fig. 5(c) is reduced by about 90%. That is, the NETD can be improved by using time-discrete modulation technology, not by increasing the illuminating energy of the imaging system.

It is obvious that some pixels in the top right area of the image appear dark, which is because these pixels are defective. That is to say, the outputs from these pixels do not carry the feature information from the object. By adopting the time-discrete modulation technology, we get image Fig. 5(c). It is obvious that the flaw in the top right area of the image gets fixed so the image is more uniform than Figs. 5(a) and 5(b). It also can be seen that the edges of the image in Fig. 5(c) are clearer because of low background noise.

The image frame sequence of a hot iron is shown in Fig. 6, when the imaging system is exposed to ambient vibration.
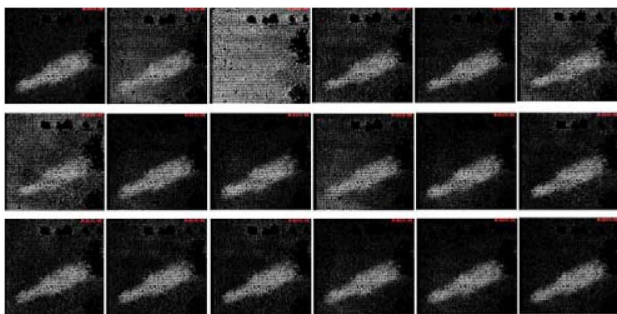

Fig. 6. Image sequence of a hot iron captured by the optical readout IR FPA imaging system without time-discrete modulation.
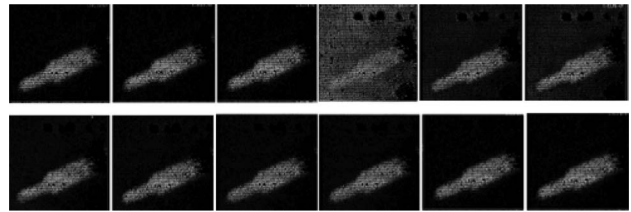

Fig. 7. Image sequence of a hot iron captured by the optical readout IR FPA imaging system with time-discrete modulation.

The first image in the image frame sequence is a normal image, and the second one is captured when the imaging system is affected by ambient impulsive vibration. The next several images include the gradually reduced noise because of the resonance of the cantilever structures of the FPA. We can see that the image goes back to normal at about the sixteenth frame. That is to say, the ambient vibration degrades the system's SNR sharply, and it will restore after about 14 frames.

The image frame sequence from the imaging system with time-discrete modulation is shown in Fig. 7, under the same ambient impulsive vibration condition.

It is obvious that there are only 3 frames that contain certain noises in the image frame sequence, so the image-recovery time is cut by more than three quarters. The experiment shows that the time-discrete modulation technique in the optical readout IR FPA imaging system can correct the image that contains the noise caused by the ambient vibration and the light fluctuations.

In conclusion, time-discrete modulation in the optical readout IR FPA imaging system is presented. This method can eliminate the background and restrain noise, which enhances the image of the optical readout IR FPA imaging system effectively. The comparative experiments show that using the time-discrete modulation technology can reduce the NETD greatly and make the images sharper. Moreover, the images are restored twice faster than without time-discrete modulation, when the imaging system is influenced by the environment vibration.

References
1. P. I. Oden, P. G. Datskos, T. Thundar, and R. J. Warmack, Appl. Phys. Lett. **69**, 3277 (1996).
2. S. Zhang, X. Hu, Y. Liao, F. He, C. Liu, and Y. Cheng, Chin. Opt. Lett. **11**, 033101 (2013).
3. A. Rogalski, Prog. Quantum Electron. **27**, 59 (2003).
4. J. Varesi, J. Lai, T. Perazzo, Z. Shi, and A. Majumdar, Appl. Phys. Lett. **71**, 306 (1997).
5. W. Qian, Q. Chen, and G. Gu, Chin. Opt. Lett. **9**, 051003 (2011).
6. P. Jia and D. Wang, Chin. Opt. Lett. **11**, 040601 (2013).
7. M. Erdtmann, L. Zhang, G. Jin, S. Radhakrishnan, G. Simelgor, and J. Salerno, Proc. SPIE **7298**, 72980I (2009).
8. Z. Duan, Q. Zhang, X. Wu, L. Pan, D. Chen, W. Wang, and Z. Guo, Chin. Phys. Lett. **20**, 2130 (2003).

9. J. Gao, Q. C. Zhang, D. P. Chen, B. B. Jiao, H. T. Shi, J. Qian, T. Cheng, and X. P. Wu, Infrared Millimeter Waves **28**, 249 (2009).

10. M. Liu, Y. Zhao, L. Dong, X. Yu, X. Liu, M. Hui, J. You, and Y. Yi, Opt. Lett. **34**, 3547 (2009).

11. X. Chu, Y. Zhao, L. Dong, Q. Jia, X. Yu, X. Liu, C. Gong, and Y. Jin, Opt. Express **20**, 9516 (2012).

12. J. Zhao, Proc. SPIE **5783**, 506 (2005).

13. H. Torun and H. Urey, Proc. SPIE **5957**, 59570O (2005).

14. J. P. Salerno, Proc. SPIE **6542**, 65421D (2007).

15. X. Wang, S. Ma, and X. Yu, Appl. Phys. Lett. **91**, 054109 (2007).

16. Y. Jin, X. Yu, Y. Zheng, Y. Zhao, X. Liu, and L. Dong, Proc. SPIE **8191**, 819102 (2011).